

## Techniques for the display and editing of marine potential field data

Projects 730081, 840056

Ron Macnab, Jacob Verhoef and John Woodside  
Atlantic Geoscience Centre, Dartmouth

Macnab, R., Verhoef, J., and Woodside, J., *Techniques for the display and editing of marine potential field data*; in *Current Research, Part A, Geological Survey of Canada, Paper 87-1A*, p. 865-875, 1987.

### **Abstract**

*Efficient editing and production of potential field maps is facilitated with tools developed for enhancement and display of large data sets. These include software packages for gridding and contouring, construction of shadowgrams, and directional filters. The clean data bases that result from applications of these techniques are basic to high level geophysical interpretation.*

### **Résumé**

*La préparation efficace et la production de cartes de champs potentiels sont facilitées grâce à des outils mis au point pour l'amélioration et l'affichage de grands ensembles de données. Ces ensembles comprennent des logiciels pour le tracé de quadrillage et de courbes de niveau, la construction d'ombrogrammes et de filtres directionnels. Les bases de données épurées obtenues après l'application de ces techniques représentent une interprétation géophysique de base à très élaborée.*

This document was produced  
by scanning the original publication.

Ce document est le produit d'une  
numérisation par balayage  
de la publication originale.

## INTRODUCTION

The Atlantic Geoscience Centre (AGC) has been compiling marine magnetic and gravity data collected by various EMR agencies off the east coast of Canada for over twenty five years (for an overview of offshore survey operations see e.g. Macnab, 1983; Miller et al., 1983; Macnab et al., 1985). The bulk of these data have recently undergone major overhaul and compilation, with a view to producing high quality regional maps and a clean data base for future reference and interpretation.

Our ability to handle large data sets has been increased by the acquisition of tools for display, manipulation, and editing. Using small and powerful micro-computers, we have streamlined many of the procedures that formerly consumed hours, and are now able to interact with our data in a manner impossible just a few years ago. A key component in this development has been the introduction of techniques for rapid graphical display, both in colour and in black and white. This is making it much easier to assess problems, and to correlate the information content of large geographic data sets.

## THE DATA

The data consist of about 2.8 and 2.3 million observations of the magnetic and gravity fields, respectively. These observations consist of numerous discrete data sets collected on separate cruises ranging over the entire east coast offshore (Fig. 90.1). They represent data densities that range from isolated ships' reconnaissance tracks to closely spaced systematic surveys. There is overlap between many of the data sets, as in situations where systematic surveys have been carried out in areas crossed previously by reconnaissance tracks, or when certain areas have been resurveyed (sometimes after intervals of several years) at closer line spacings.

The quality of this data base is dependent on the accuracy of individual observations. The accuracy of the data is affected by a number of measurement, positioning, and processing errors. Obvious errors, like spikes are easily detectable. However, subtle inaccuracies in a large data set can better be dealt with through application of techniques like those described here.

Errors in the magnetic measurements are caused by short-term changes of the magnetic field (diurnal variations and storms), navigational inaccuracies, and failure or misapplication of the International Geomagnetic Reference Field (IGRF) to model adequately the long-term secular variation. Although the most current representations of the reference field (IAGA Division 1 Working Group 1, 1986) are considerably better than the older ones (IAGA Division 1 Working Group 1, 1981), we found that there remains a small time-dependent factor (work in progress).

Major errors in gravity measurements arise from failure to properly account for ship's course and speed; these need to be observed accurately in order to calculate the Eotvos correction. Other problems arise from environmental and instrumental factors, e.g. accelerations introduced by ship's re-

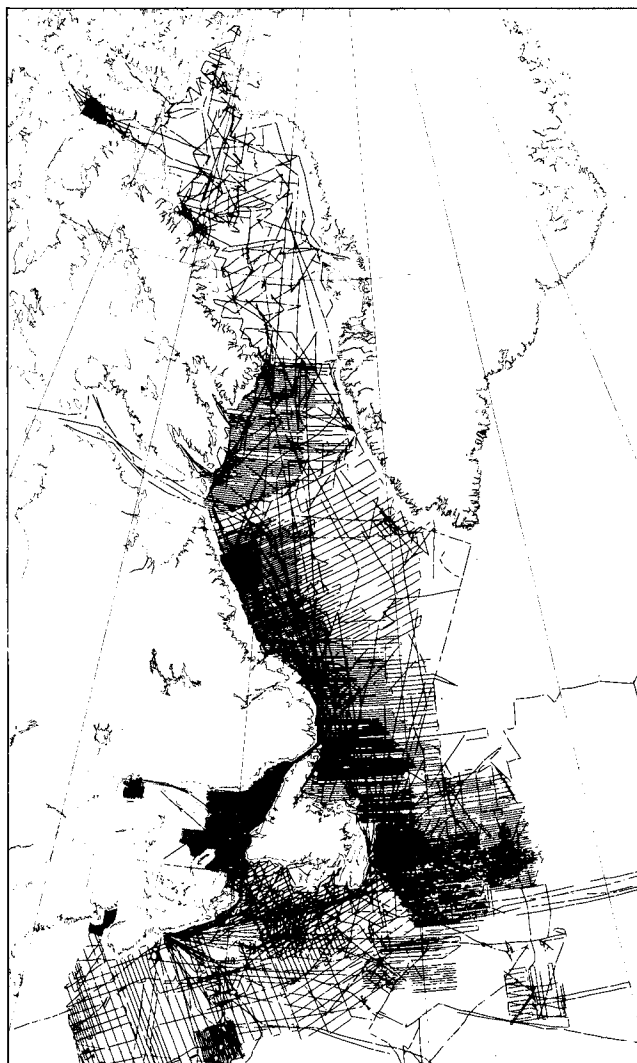


**Figure 90.1.** Track chart showing the coverage of magnetic and gravity measurements off Eastern Canada.

sponse to wave motion, slow changes in the mechanical or electrical characteristics of the gravimeter, etc. A third class of error arises from mis-ties to the land gravity reference network.

Whether in magnetics or gravity, the errors share a similar effect, which is to introduce disagreement between observations along intersecting or closely-spaced ships' tracks. Without automated techniques, the identification and correction of these problems can be a time-consuming and error-prone operation.

## GRIDDING AND CONTOURING

The first step in data processing is to convert irregularly-spaced ship track data into observations distributed over a regular grid. For this, an automated gridding routine is

applied which is a combination of an adjustable digital filter with a weighting method (Slootweg, 1978, Verhoef et al., 1986). The method produces grid values that are unbiased by track-line geometry, and also diminishes the influence of residual positioning errors. It has the disadvantage that along-track details with wavelengths shorter than the mean track spacing are lost.

Computer contouring is accomplished in three steps:

- 1) generating a square grid over the area to be contoured;
- 2) estimating the mesh point values for this grid from the data point values;
- 3) drawing contour lines using the mesh point values.

The spatial filter used in the calculation of mesh point values from unevenly spaced data is a low-pass Butterworth filter of the first order, which reduces the short wavelength components in the data. The choice of the cut-off wavelength of this filter depends on the data point distribution and the expected spectral content of the variable to be contoured.

In general, marine survey operations yield sets of observation points with an irregular distribution: data points tend to be more closely spaced in along-track than in cross-track directions. Careful specification of filter constants should minimize the effects of this sort of data distribution, while predicting how much filtering will occur for any given wavelength.

If too low a cut-off wavelength is selected for the filter, the coherent structure of the resulting contour lines will be disturbed by irregularities in the data distribution. If on the other hand the cut-off wavelength is chosen too high, short wavelength detail will not appear in the contours. Thus an optimum value has to be established which will depend on the mean distance between tracks. If this mean distance varies largely over an area, the gridding can be done in subareas with different filter settings, and the resulting grid files merged by means of a simple averaging technique. However, in this case the resulting grid will be spectrally inhomogeneous.

Our current gridding procedure for the routine handling of track data uses as input the original time-sequential field observations, each tagged with latitude and longitude coordinates. The output consists of a grid file representing a matrix of mesh points separated by equal increments of latitude and longitude.

The grid file contains three quantities for each mesh point:

- a) the summation of the values of the contributing data points multiplied by the weighting function;
- b) the summation of the weight function;
- c) the number of contributing data points.

Data points contribute to a grid value whenever the weight function, which is a function of the distance between the data point and the grid point, is higher than 0.3% of its maximum value. This maximum value occurs when data point and grid point coincide.

The gridding operation consists first of scanning and multiplying all data points by the appropriate weighting

function for each grid point, with summations stored in the grid file as quantities a), b), and c) defined above. The value at each grid point is then calculated by dividing summation a) for that location by the corresponding total weight function b). If the number of data points contributing to one grid point is less than a set limit, a flag-value is stored indicating 'no data'.

Storing quantities a), b), and c) separately for each grid point makes it easy to update the grid file whenever new data are available, or to enter corrections for bad data. For instance, suppose that after contouring one observes several contour lines which are obviously disturbed by a series of erroneous values along a particular track. Eliminating these bad values is easily accomplished by re-running the gridding program on a synthetic track that matches the location of the bad track, but with signs reversed on all the offending data points. The weight functions are adjusted accordingly in the appropriate grid locations. Note that it is not necessary to re-grid the entire set of data to enter corrections for any given track segment.

The actual contour map is produced by drawing line segments within the elementary grid squares. The end points of these segments are found by linear interpolation between the mesh points. Other options are to display contours as changes in colour or line pattern. In this case the locations of the changes are also found by linear interpolation between the mesh points.

## **FILTER EFFECT OF THE GRIDDING AND CONTOURING PROCESS**

A cut-off wavelength of 20 nautical miles appears to be the optimum for the total set of magnetic and gravity observations collected by AGC. This means that at 20 nautical miles from a mesh point the weights are 6 dB down (or approximately 70 %), decreasing further with increasing distance. In areas of smaller than average track spacing, this filter setting results in the loss of some detail.

This filter effect is illustrated in Figure 90.2, where the solid line represents observed magnetic anomalies along a short segment of ship's track. The dotted line shows the anomalies reconstituted from gridded values along the same track. The filter effect is clearly seen as an attenuation of the short wavelength anomalies. The effect is less pronounced for gravity observations, because the gravity field varies less over similar distances than the magnetic field.

Note that the dotted profile in Figure 90.2 displays a slight level shift. This might be the result of biases in the observed data, or it might be introduced from adjacent lines; the grid file contains influences from both sources.

The technique of comparing values observed along track with reconstituted grid values can also be applied to locate track segments that agree poorly with their neighbours. The average differences between observed and reconstituted values should yield random residuals for short wavelength anomalies over a number of points with no bias. However,

STARTING POINT: 49.65 N, 51.58 W  
END POINT: 48.29 N, 51.42 W

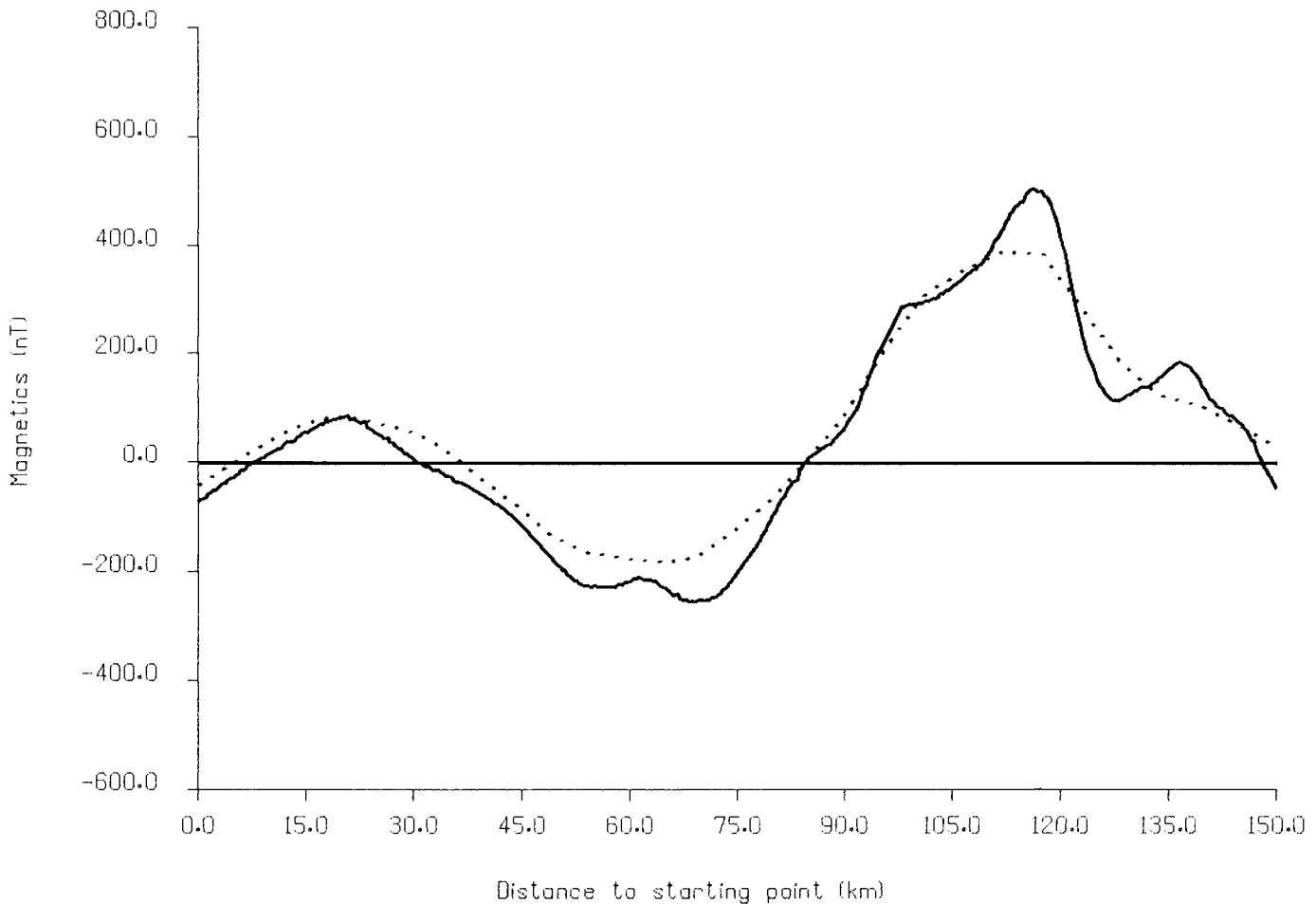


**Figure 90.2.** Filtering effect of the gridding routine. The continuous line represents the observed magnetic anomalies along a track of a 1979 cruise. The discontinuous line gives the anomalies along the same track, but now recalculated from the gridded values. The filter effect of the gridding, for which a Butterworth filter with a 20 nautical mile cut-off wavelength was used, is clearly seen as the attenuation of the short wavelength anomalies. The profile is located to the east of Newfoundland.

where a track segment agrees poorly with its neighbours, the residuals may be expected to have a consistent sign.

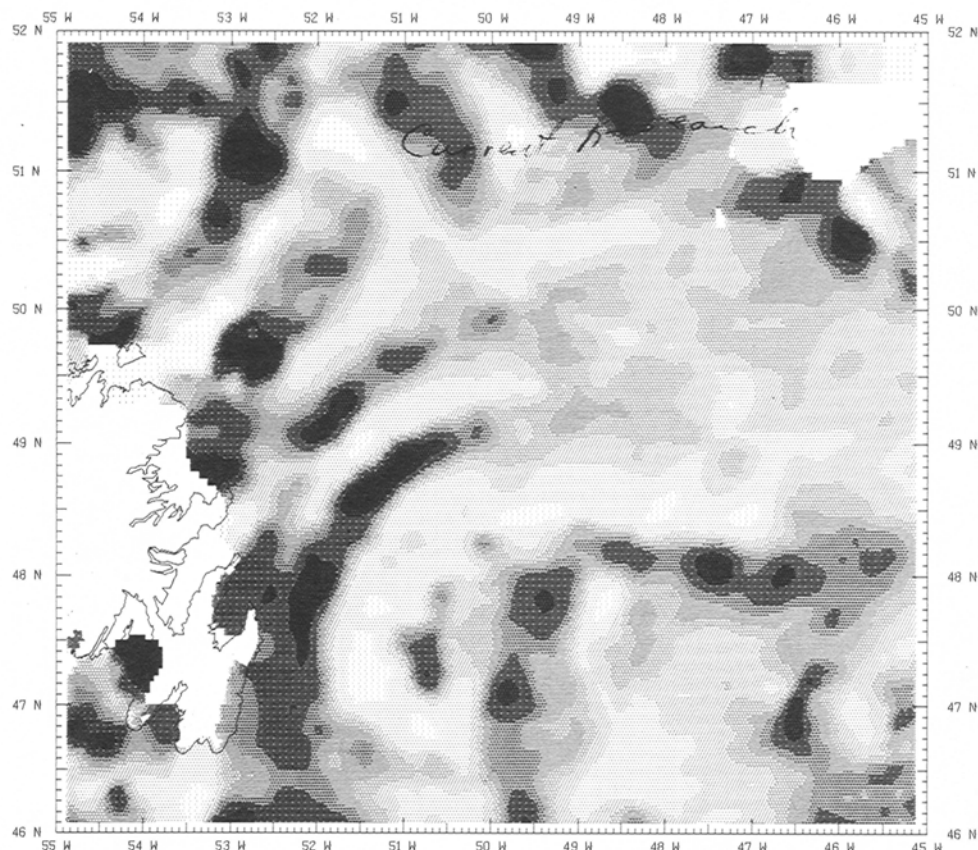
## SHADOWGRAMS

Data presentation by way of a contour map has the disadvantage that features with amplitudes smaller than the contour interval may get lost. One solution is to present a three-dimensional view of the grid values. Another solution is to present slopes instead of values. The latter approach is easy to implement by calculating and plotting the directional derivative of the grid values. The direction of this derivative is user selectable, and depends on the slopes one wants to enhance (e.g. Verhoef et al., 1986).

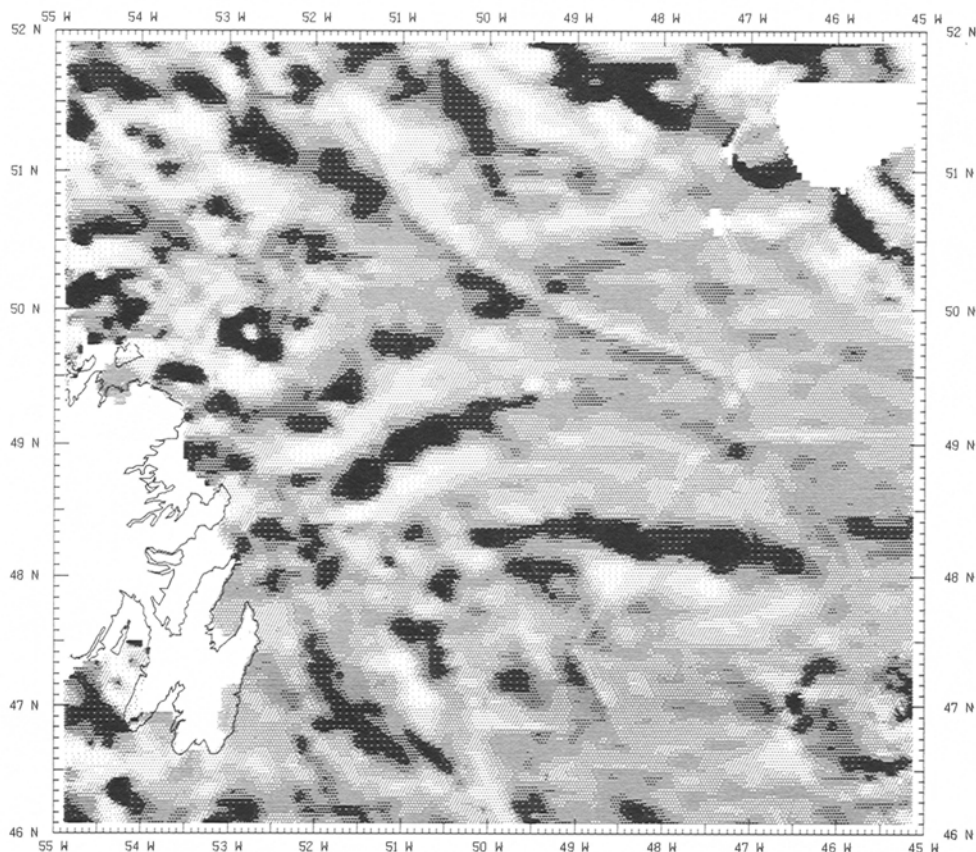
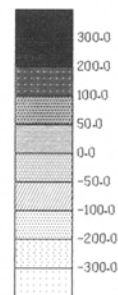
The resulting plot suggests the shadows that would be obtained by shining light across the surface of the gridded data from a given direction. An advantage of this presentation is that one obtains a better resolution, due to the relative increase in power of the shorter wavelengths caused by the application of the directional derivative. Bad tracks are therefore more easily detected.

As an illustration of the method, we describe below a specific application of the shadowgram method to identify bad data in a subset of AGC data located northeast of Newfoundland.

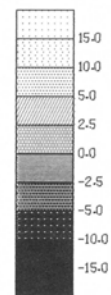
Figure 90.3a is an anomaly map derived from marine magnetic observations. Clearly visible are the arcuate trends



**Figure 90.3a.** Magnetic anomalies in an area to the north-east of Newfoundland. Clearly visible are the arcuate trends of the strong positive anomalies of the Avalon basement across the Grand Banks. The data include a 'bad track' which hardly shows.



**Figure 90.3b.** Shadowgram of the magnetic anomalies of Figure 90.3a in the direction of 210°, i.e. 30° west of south. The values plotted are the slopes (unit is nT/km) of the anomalies. The 'bad track' shows the irregular zigzag feature tracking from the northern edge of the map to a point near the southern edge.



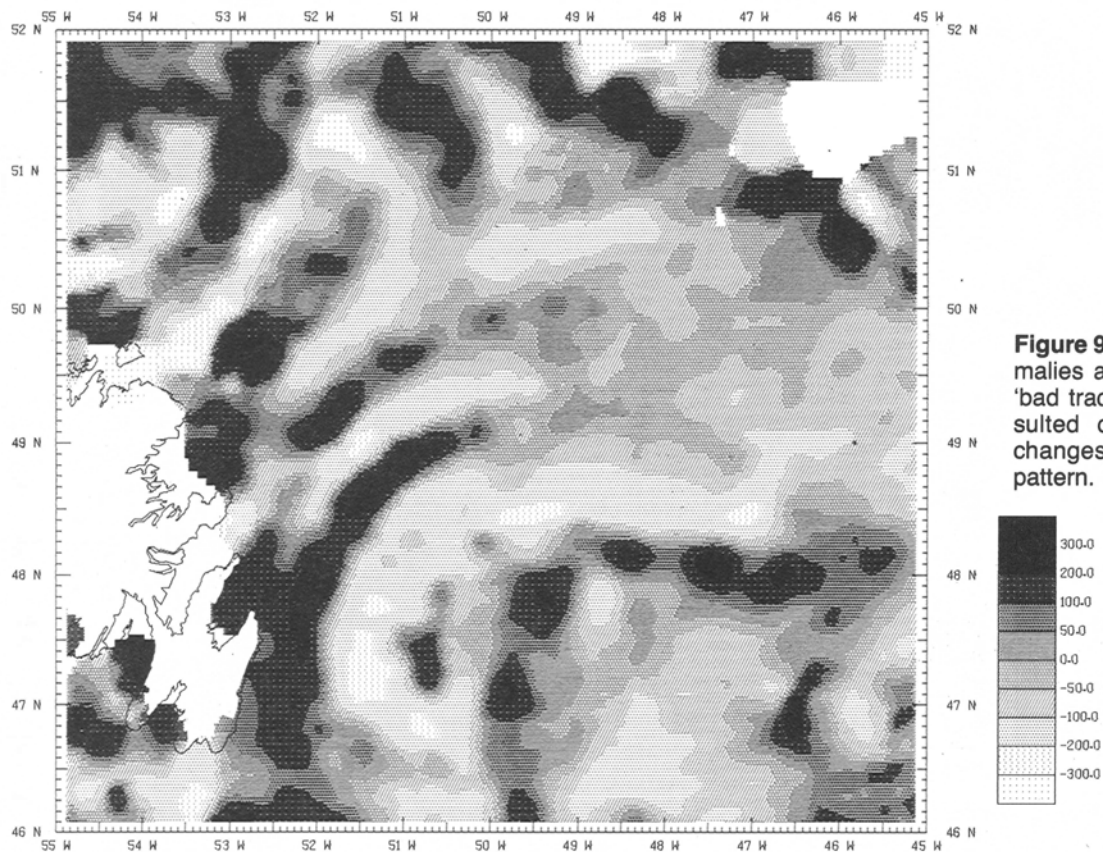


**Figure 90.3c.** Magnetic anomalies after correcting for the 'bad track'. The correction resulted only in some minor changes in the anomaly pattern.

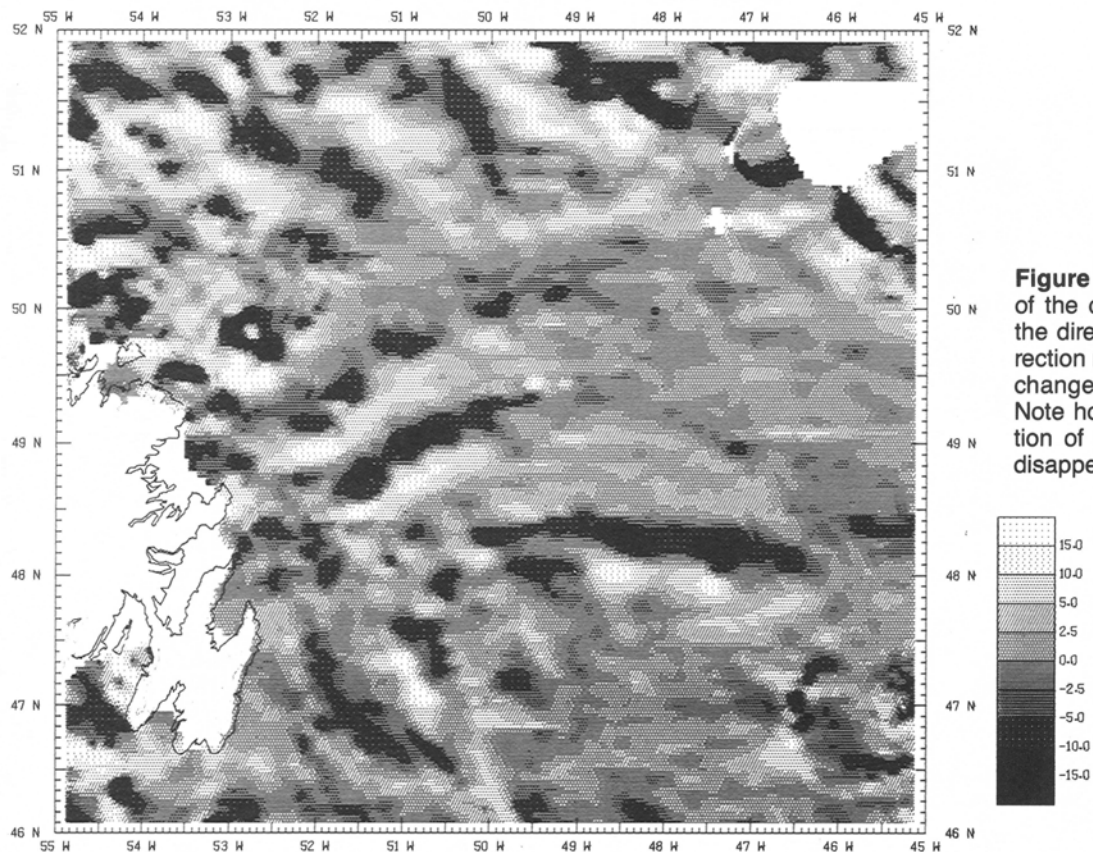


**Figure 90.3d.** Shadowgram of the corrected anomalies in the direction of 210°. The correction resulted in a significant change in the shadowgram. Note how the dominant lineation of Figure 90.3b has now disappeared.



of the Avalon basement across the Grand Banks and continuing into Orphan Basin (e.g. Haworth, 1980), where they decrease in amplitude. This map contains an erroneous track segment, although even a careful inspection of the contours does not reveal anything seriously amiss.

Figure 90.3b is a shadowgram of the same area, with the source of illumination at  $210^\circ$  (i.e.  $30^\circ$  west of south). Even a cursory glance suffices to detect an irregular zigzag feature tracking from the northern edge of the map to a point near the southern edge. An inspection of the ship tracks in the area shows that this feature indeed corresponds to an identifiable track segment.

The gridded data set can now be recalculated using a synthetic correction track as outlined above, to eliminate the effect of erroneous data. Figure 90.3c is the corrected magnetic anomaly field, which differs little from the uncorrected field. The corrected shadowgram in Figure 90.3d, however, clearly shows the improvement in the data set. The data base will likewise be cleaner following the correction.

The shadowgram technique was applied to the entire magnetic data set using various directions of illumination, in order to locate and identify erroneous track segments in different directions. Synthetic correction tracks were then fed into the gridding process to eliminate bad data. This resulted in the elimination of about 3% of the data set, and led to a significant improvement in the final magnetic anomaly map. This map will be published at 1:5 000 000 in a forthcoming *Geology of Canada* volume, together with corresponding maps of gravity, bathymetry and geology.

## EDITING GRAVITY DATA FOR NESS MAPS

Editing of gravity data prior to publication as maps in the National Earth Science Series (NESS) is facilitated using some of the techniques described in this paper. Normally, someone must painstakingly examine all the posted values on each of twelve preliminary 1:250 000 scale maps which cover the area of a 1:1 000 000 NESS map. The search is for segments of data which are inconsistent with the surrounding data.

A series of graphical displays may be quickly and effectively used as an aid in finding erroneous data without the need to scan visually the entire set of posted values. Erroneous data show up, for example, on contour plots as "herring-bone" patterns where a track segment is shifted with respect to its neighbours or as "bull's eyes" when a spike is present. As noted above, they may be identified on shadowgrams as track-correlated bands, or by comparison of raw observed data with gridded values to determine if data are suspiciously different from the local field.

A systematic procedure is followed in the validation of data destined for the NESS maps. The criteria used are: line-to-line contourability of the data, consistency of crossover values, continuity between sheets, variability along north-south lines (where the Eotvos correction is notoriously diffi-

cult to determine), and compatibility of short unconnected track segments. A least squares adjustment of the gravity data optimizes crossover variations, and ensures that the data set is clear of drift and levelling variations. What remains to be done therefore is primarily the finding of data which have escaped this treatment, because they were not properly connected into the adjustment network. For each of the twelve subsets of a NESS sheet the data are plotted as shadowgrams and contours and compared automatically with filtered and gridded data. Visual checks of problem areas can then be made.

## DIRECTIONAL FILTERING

Some parts of the magnetic data feature corrugations that are obviously due to level differences between adjacent and parallel ship tracks.

An example is shown in Figure 90.4a, which illustrates the magnetic anomaly field to the east of Nova Scotia. The East Coast Magnetic Anomaly (ECMA) is clearly visible as a strong positive feature running from about  $41.5^\circ\text{N}/65^\circ\text{W}$  to  $43.5^\circ\text{N}/59.5^\circ\text{W}$ , while a few subtle NNW-SSE lineations can be seen in the lower part of the map area. These lineations are more clearly visible in the shadowgram of Figure 90.4b, which has been constructed with a direction of illumination of  $90^\circ$ . An inspection of the track lines in Figure 90.1 indicates several track segments in the area with a similar spacing and orientation; the lineations in the magnetic field are obviously related to these tracks, and are probably caused by levelling problems in the data.

One method for correcting levelling errors uses differences between tracks at crossovers. Data adjustments required to minimize these differences in a least squares sense are then used to adjust all the observations. This technique is well suited for adjusting gravity survey data, and has been applied to the gravity data using 21,813 crossovers (Earth Physics Branch, 1986). However, it is difficult to apply on observations of a time varying field like the magnetic field, when the period over which observations have been made is so long that time-dependent factors still remain after a first correction.

In the particular case of corrugations in the magnetic field, an effective approach involves the directional filtering technique.

From an examination of the shadowgram in Figure 90.4b and the track lines in Figure 90.1, it is obvious that the NNW-SSE lineations in the magnetic field will produce relatively high values in that direction of the power spectrum, with a wavelength determined by the track spacing. Figure 90.5 is the two-dimensional power spectrum of the data in this particular area, obtained by applying a 2D Fourier Transform to the gridded data.

In simple terms the power spectrum shows the variation of the square of the amplitude of the magnetic anomalies with their wavelength. In addition to the general decay of the power going from longer to shorter wavelengths, there is some local increase in the power along the direction of  $55^\circ$ .

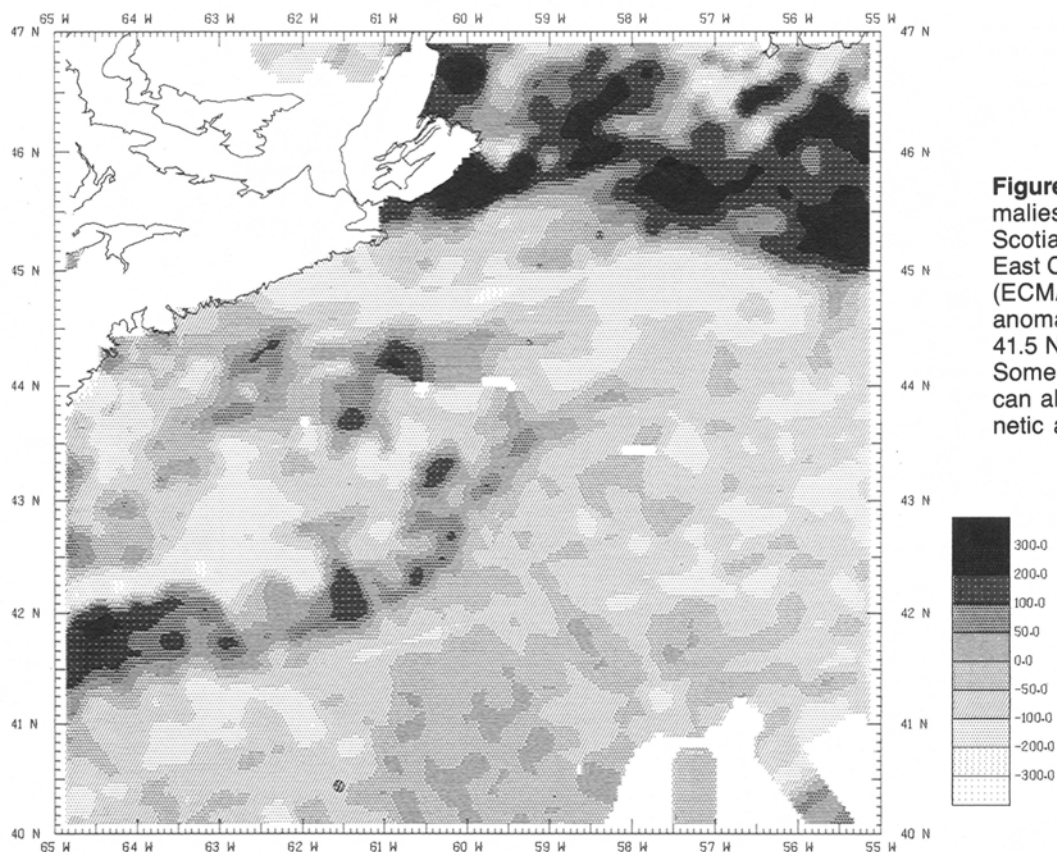


**Figure 90.4a.** Magnetic anomalies to the east of Nova Scotia. Clearly visible is the East Coast Magnetic Anomaly (ECMA) as a strong positive anomaly running from about 41.5°N/65°W to 43°N/59.5°W. Some NNW-SSE lineations can also be seen in the magnetic anomalies.

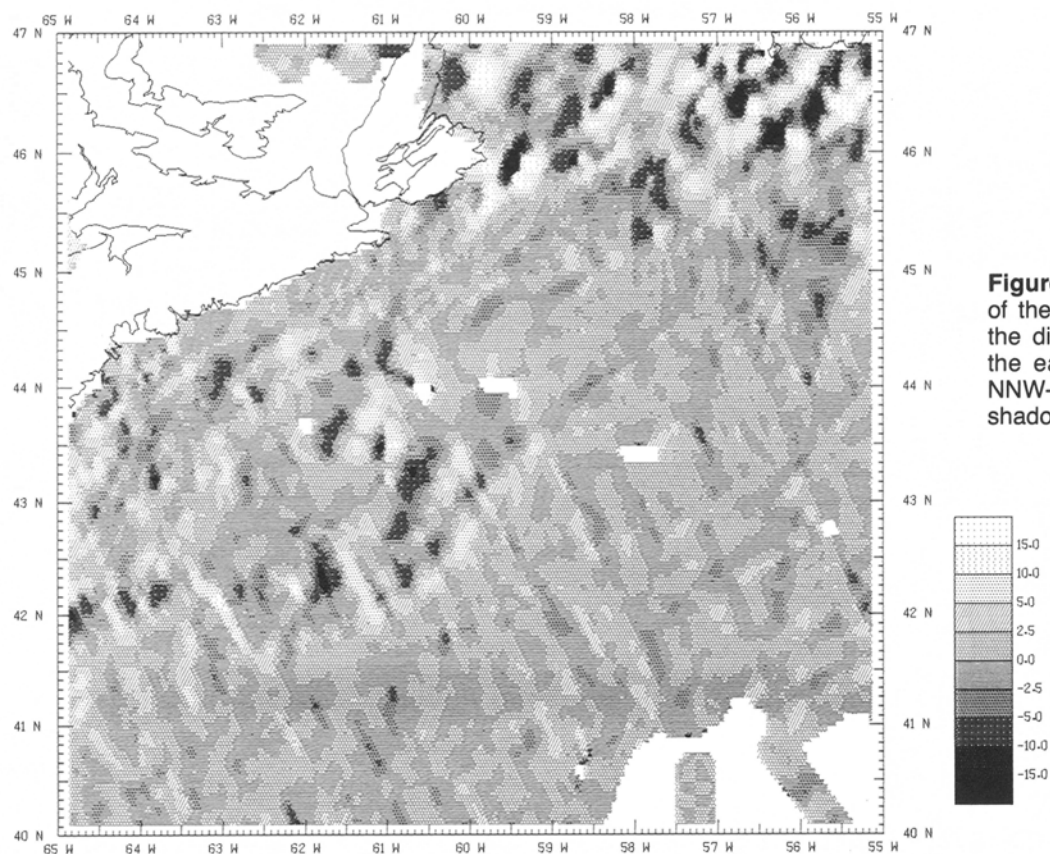


**Figure 90.4b.** Shadowgram of the magnetic anomalies in the direction of 90°, i.e. from the east. Note the dominant NNW-SSE lineations in the shadowgram.



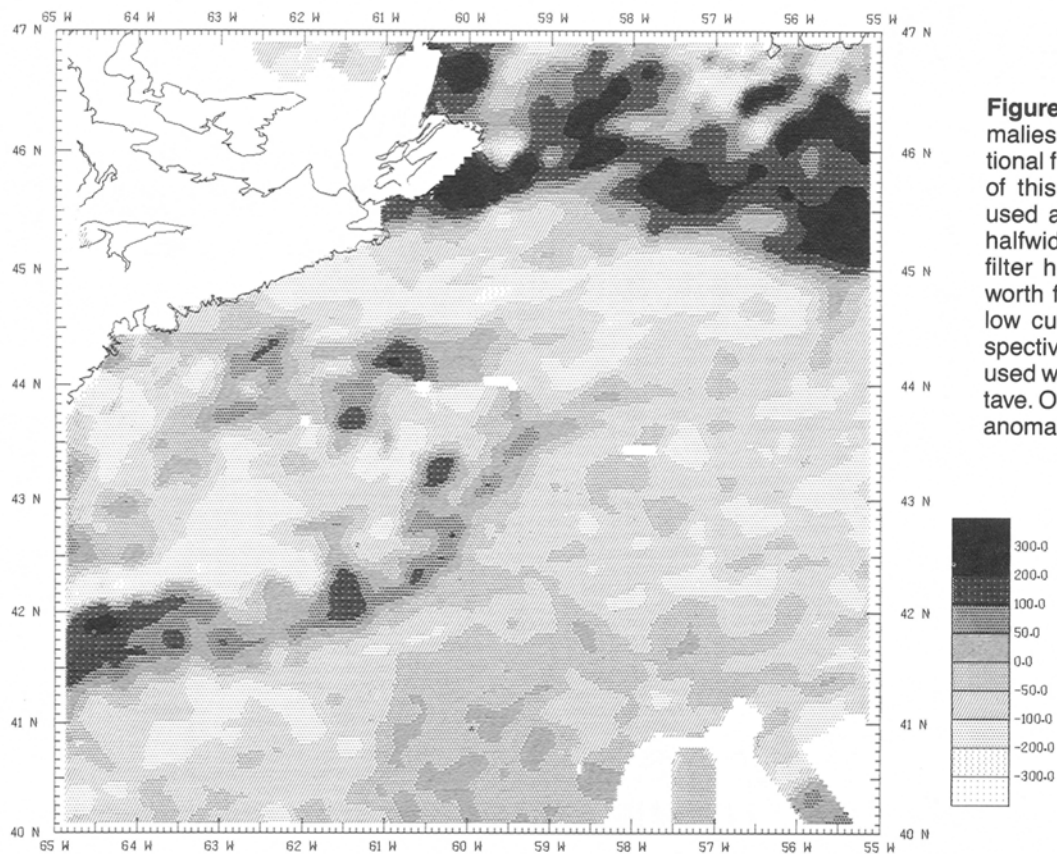


**Figure 90.4c.** Magnetic anomalies after applying a directional filter. The directional part of this filter is Gaussian; we used a direction of  $55^\circ$  and a halfwidth of  $20^\circ$ . In addition the filter has a bandpass Butterworth filter for which high and low cutoff wavelengths of respectively 18 and 65 km were used with a roll-off of 48 dB/octave. Only small changes in the anomaly pattern can be seen.

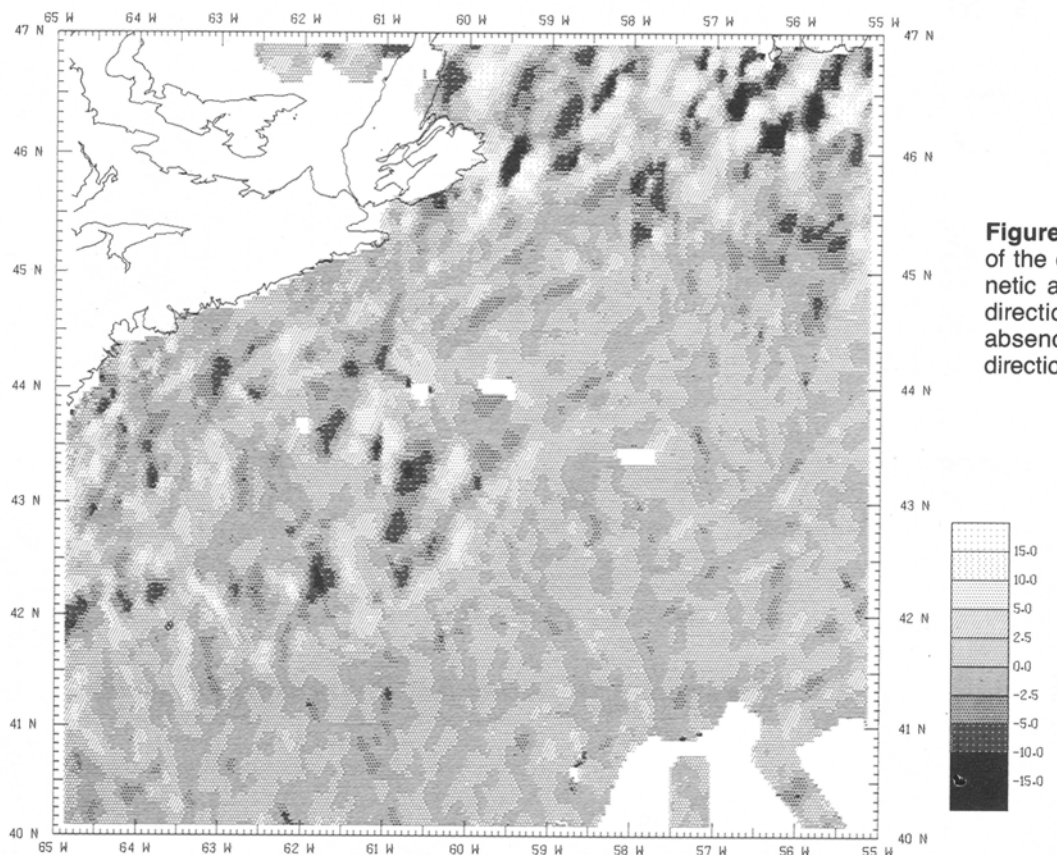


**Figure 90.4d.** Shadowgram of the directional filtered magnetic anomalies, again in the direction of  $90^\circ$ . Note the absence of the NNW-SSE directions.

This shows up as a series of small spots in the figure, extending from the centre along the 055-235 axis (see line indicated by arrows in Fig. 90.5).

The picture becomes clearer if we calculate the power spectrum at an azimuth of  $55^\circ$  (Fig. 90.6). The power in this direction and between wavelengths of 18 and 65 km is larger

than the corresponding power in other directions. This indicates a relationship between lineations in the field, and the spacing and orientation of the tracks.

In order to isolate anomalous features in the power spectrum, it is possible to define a mean spectrum by averaging over the different directions, and then to look at the deviations

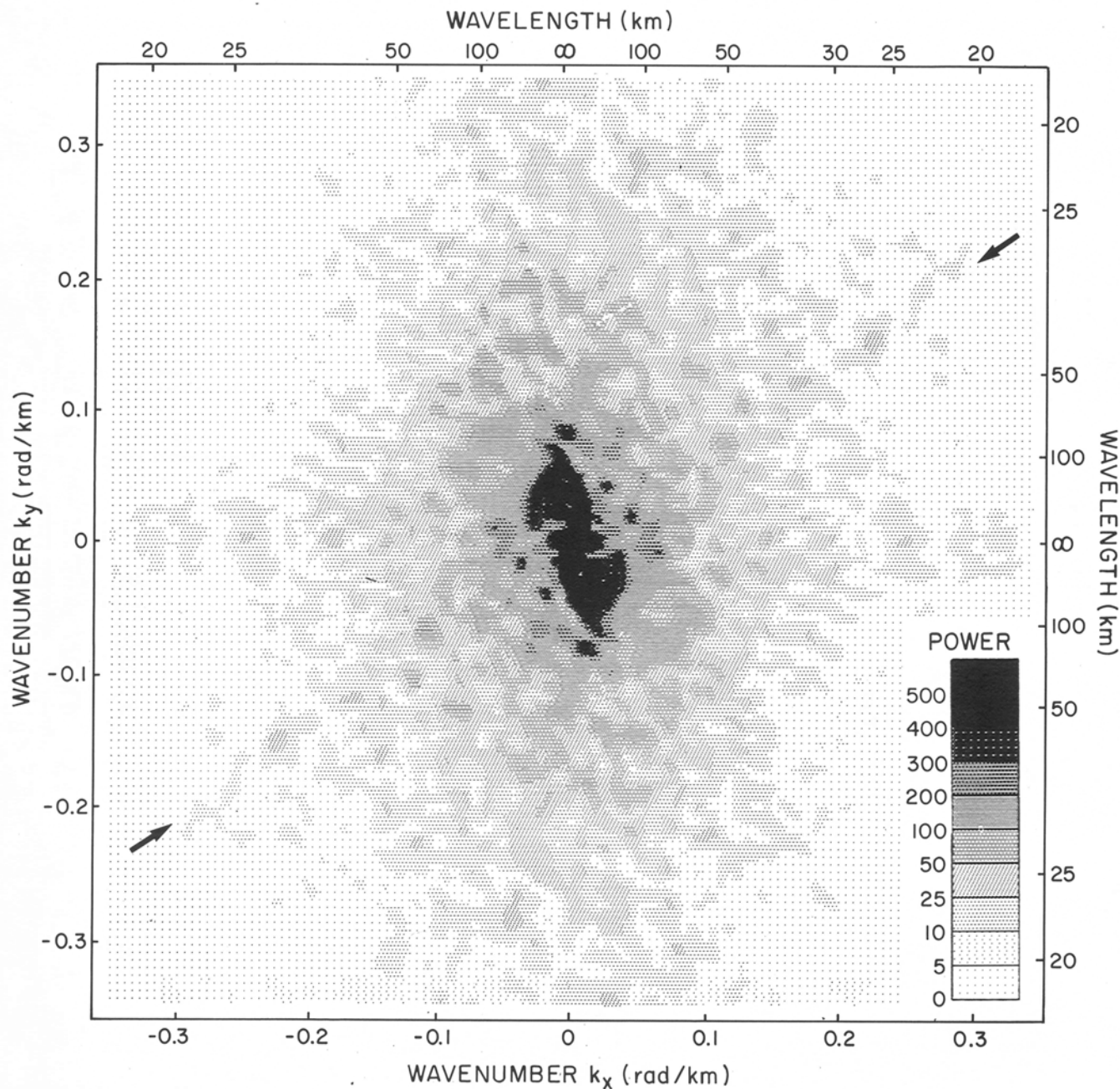


**Figure 90.5.** Two-dimensional power spectrum of the magnetic anomalies of Figure 90.4a. Before applying a 2-D Fourier Transform to the data, a best fitting plane was subtracted from the data and a cosine taper was applied. The wavenumber in the x-direction is shown along the horizontal axis, while the wavenumber in the y-direction runs along the vertical axis. As the input data were a real function the spectrum shows some symmetry: the first and third quadrant are the same, as are the second and fourth. For presentation purposes wavelengths of less than 18 km are not shown. The arrows gives the 055° direction.

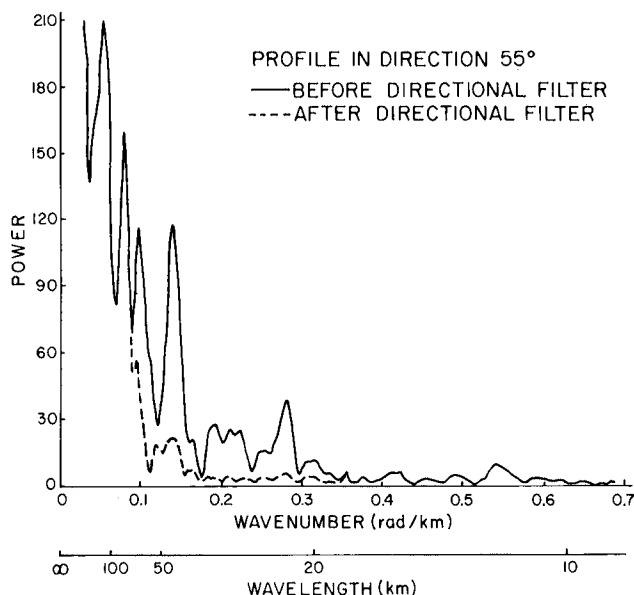


**Figure 90.6.** Power spectrum in the direction of  $55^\circ$ . The continuous line gives the power spectrum of the original anomalies. The dashed line gives the power spectrum in the same direction after applying a directional filter. Note the relatively high power between wavenumbers 0.36 and 0.12 in the original power spectrum, which was taken out by the directional filtering.

from these averages (e.g. Simpson et al., 1986). However, the power spectrum of magnetic anomalies in general is not axially symmetric like that obtained from gravity anomalies; it has instead an elliptical shape due to the vectorial character of the magnetic anomalies.

To reduce the effect of mislevelling between tracks and hence to eliminate the lineations in the magnetic field, we reduce the power in the direction of  $55^\circ$  by applying a directional filter. The procedure we follow is to use a filter with a directional part which is Gaussian; the effective width of this filter is defined by a halfwidth specification. In addition to a directional component, the filter includes a Butterworth wavelength bandpass. We used cut-off wavelengths of 18 and 65 km for the bandpass filter, and a roll-off of 48 dB/octave.

The dotted line in Figure 90.6 shows the power in direction  $055^\circ$  after the directional filter has been applied. Figure 90.4c shows the magnetic anomalies in the area after applying the directional filter, with the corresponding shadowgram in Figure 90.4d. There has clearly been an improvement in the data set, especially in the NNW-SSE direction.

The method described above demonstrates how levelling problems can be eliminated by using a directional filter. However, the use of such a filter also eliminates genuine power in the specified direction. We are investigating different approaches to resolve this loss of information. One approach is to use the power in the direction of corrugation to define level corrections that are applied directly to observed data along selected tracks.

## ACKNOWLEDGMENTS

The computer programs described and applied here were developed at the Marine Geophysical department of the Vening Meinesz Laboratory at the Rijksuniversiteit at Utrecht, the Netherlands. The acquisition, processing and compilation of data would not have been possible without the active collaboration, at various stages, of a number of groups and individuals within the GSC (Geophysics Division) and in other departments (Canadian Hydrographic Service). Wayne Prime, Gordon Oakey, and Keh-Gong Shih were instrumental in wrestling large data sets into the excellent shape in which they are now. We thank B.D. Loncarevic and F. Marillier for reviewing this paper.

## REFERENCES

### Earth Physics Branch

- 1986: Integration of Atlantic Geoscience Centre Marine Gravity Data into the National Gravity Data Base; Earth Physics Branch Open File 85-32, Joint Publication of Earth Physics Branch and Atlantic Geoscience Centre.

### Haworth, R.T.

- 1980: Appalachian structural trends northeast of Newfoundland and their trans-Atlantic correlation, *Tectonophysics*, v. 64, p. 111-130.

### IAGA Division 1 Working Group 1

- 1981: International Geomagnetic Reference Fields: DGRF 1965, DGRF 1970, DGRF 1975 and IGRF 1980, EOS, Transactions of the American Geophysical Union, v. 62, p. 1169.  
1986: International Geomagnetic Reference Field Revision 1985, EOS, Transactions of the American Geophysical Union, v. 67, p. 523-524.

### Macnab R.F.

- 1983: Multiparameter mapping off the east coast of Canada, in *Current Research, Part A*, Geological Survey of Canada, Paper 83-1A, p. 163-171.

### Macnab R.F., Loncarevic B.D., Cooper R.V., Girouard P.R., Hughes M.D. and Shouzhi F.

- 1985: A regional marine multiparameter survey south of Newfoundland, in *Current Research, Part B*, Geological Survey of Canada, Paper 85-1B, p. 325-332.

### Miller R.O., Macnab R.F., Amos C.L. and Fader G.B.

- 1983: Canadian East Coast multiparameter surveys, 1982, in *Current Research, Part B*, Geological Survey of Canada, Paper 83-1B, p. 331-334.

### Simpson R.W., Jachens R.C., Blakely R.J. and Saltus R.W.

- 1986: A new isostatic residual map of the conterminous United States with a discussion on the significance of isostatic residual anomalies, *Journal of Geophysical Research*, v. 91, p. 8328-8372.

### Slootweg A.P.

- 1978: Computer contouring with a digital filter; *Marine Geophysical Researches*, v. 3, p. 401-405.

### Verhoef J., Collette B.J., Miles P.R., Searle R.C., Sibuet J.-C. and Williams C.A.

- 1986: Magnetic anomalies in the northeast Atlantic Ocean; *Marine Geophysical Researches*, v. 8, p. 1-25.